PAPER

Check for updates

Nano-hydroxyapatite (n-HAP) from *Pangasius* bone side streams and its application as a reinforcing agent in biodegradable food packaging films

Oshin Kawduji Thool,[a] Abhilash Sasidharan, [ID] *[a] Bindu M. Krishna,[b] Sarasan Sabu,[c] Muhammed Navaf[d] and Kappat Valiyapeediyekkal Sunooj[d]

The bone side streams from catfish (*Pangasianodon hypophthalmus*) were used to produce nano-hydroxyapatite (n-HAP) by a calcination method. Bones were de-proteinized and calcined at 500, 700, and 900 °C at 2, 4, and 9 h, pulverized and cooled. Inductively coupled plasma (ICP-OES), Fourier Transform Infrared (FTIR) spectroscopy, X-ray diffraction (XRD), and Transmission Electron Microscopy (TEM) were used to characterize the trace elements, functional groups, phase formation, and morphology of n-HAP, respectively. Using ICP-OES, an atomic ratio of 1.56 Ca/P was found in catfish bone calcined at 900 °C for 9 h. The FTIR spectra of the sample calcined to the same degree were matched with the standard hydroxyapatite FTIR spectrum. A high crystallinity of 99.5% was confirmed by XRD measurements as the calcination temperature and duration were increased. TEM analysis revealed that the n-HAP crystals have an average size of 71.38 nm. Cassava starch–n-HAP reinforced composite films were prepared with varying n-HAP concentrations which resulted in minor variations in the film thickness ranging from 0.05 to 0.16 mm. The control film exhibited a tensile strength (TS) value of 12.5 MPa while the maximum TS value of 16.10 MPa was exhibited by the sample with 0.8% n-HAP. The lowest elongation at break value was reported for the control film (1.55%) and the maximum (6.87%) was reported for the sample with 0.4% n-HAP. The film incorporating 0.8% n-HAP showed the highest seal strength while the water vapor transmission rate (WVTR) of the composite films reduced from 3.59×10^{-1} g Pa^{-1} m^{-1} s^{-1} to 1.67×10^{-1} g Pa^{-1} m^{-1} s^{-1} as n-HAP concentration increased. The film incorporating 0.4% n-HAP showed identical WVTR values to those of the film with 0.8% n-HAP. These results showed that the n-HAP-incorporating films exhibited better mechanical and barrier properties compared to the control film.

Sustainability spotlight

In the quest for sustainable materials and practices, researchers and industry leaders are turning to innovative solutions that address both environmental concerns and practical needs. One such breakthrough is the development of nano-hydroxyapatite (n-HAP) derived from *Pangasius* bone side streams, a byproduct of fish processing. Nano-hydroxyapatite (n-HAP) is a bioceramic material that mimics the natural bone mineral component hydroxyapatite (HAP). It possesses excellent mechanical properties, biocompatibility, and biodegradability. One of the most promising applications of n-HAP is in the realm of biodegradable food packaging films. The incorporation of n-HAP into these films provides several benefits. Research has shown that adding n-HAP to starch-based films enhances their tensile strength and elongation properties, making them suitable for various food packaging applications. As more fish processing facilities adopt this practice, the availability of n-HAP could increase, leading to more widespread use in packaging and other sustainable materials. Additionally, ongoing research aims to further optimize the performance of n-HAP in different types of biodegradable polymers and explore new applications.

1 Introduction

Nowadays, more and more fish is processed once it is caught instead of being sold whole. A large number of byproducts are produced during the further processing of fish to create fillets, which are often the primary product of fish. These byproducts may make up as much as 70% of the weight of the fish.[1] A variety of procedures are involved in the post-harvest preparation of fillets, but they all entail the removal of the backbone, guts,

[a]*Department of Fish Processing Technology, Kerala University of Fisheries and Ocean Studies, Kerala, India. E-mail: drabhilash@kufos.ac.in*

[b]*Sophisticated Test and Instrumentation Centre, Cochin University of Science and Technology, Kerala, India*

[c]*School of Industrial Fisheries, Cochin University of Science and Technology, Kerala, India*

[d]*Department of Food Science & Technology, Pondicherry University, Puducherry, India*

head, fins, and skin.[2,3] Furthermore, large volumes of cut-offs are produced during automated filleting, and these and other byproducts indicate the potential for more effective use with the goals of circular utilisation and value-addition. The majority of the fish side streams produced now are used to produce underappreciated goods like biodiesel, fertiliser, and animal feed.[4,5] Biopolymers from organic waste and seafood side streams have attained considerable attention recently owing to their biodegradability, biocompatibility, low toxicity, and renewable properties.[6] The non-biodegradable nature of conventional petroleum plastics has raised serious environmental concerns worldwide, and this in turn has created an increasing need for replacing synthetic materials with eco-friendly and biodegradable substitutes.[7] Hydroxyapatite is a natural bio-ceramic material that constitutes about 60% of bone tissue.[8] Its composition is comparable to that of human hard tissues, teeth, and bones.[9] In recent times, the inclination for production of hydroxyapatite in nano form has more preference due to its biocompatible nature, enhanced surface area and resemblance to natural apatite.[10]

The nano form of hydroxyapatite (n-HAP) has found numerous applications in the fields of drug delivery, dental implant coatings, and bone tissue engineering,[11,12] among others. Hydroxyapatite could be isolated from natural sources like eggshells, coral reefs, fish, poultry, and mammalian bones. Mammalian and poultry bone side streams are widely used for collagen preparation.[13] fish bone is, in particular, of interest as an average seafood processing operation generates around 15% of bone side stream.[14]

Bones from fishes such as carp (*Cyprinus carpio*), Atlantic salmon (*Salmo salar*), tilapia (*Oreochromis niloticus*),[15] rohu (*Labeo rohita*),[16] swordfish (*Xiphias gladius*), tuna (*Thunnus thynnus*),[17] seer fish (*Scomberomorus commersonii*),[18] and catfish (*Pangasianodon hypophthalmus*)[19] have been utilized to produce n-HAP using a calcination method with promising results. *Pangasius* catfish (*Pangasius hypophthalmus*) is among the most cultured fish species of the world and is in huge demand among seafood customers.[20] *Pangasius* bone waste has been utilized in a few studies for the production of n-Hap using the thermal calcination technique.[21,22]

Various methods have been used for the production of n-HAP, including wet-chemical precipitation, solvothermal, solid-state reaction, sol–gel, emulsion, and micro-emulsion methods.[23–25] Calcination is another process employed for n-HAP extraction involving heating at higher temperatures for longer periods making it one of the less complicated methods.[26] Hydroxyapatite prepared through calcination has been reported to have a Ca/P ratio of 1.654 which is closer to the quality ratio of pure hydroxyapatite of 1.667.[22]

Hydroxyapatite used in food packaging has garnered attention due to its bioactivity, non-toxicity, and potential to enhance mechanical properties, barrier properties, and antimicrobial activity in packaging materials. It can also improve barrier properties against oxygen and moisture. A study by Zhang *et al.* indicated that n-HAP reinforced polyvinyl alcohol (PVA) films had significantly reduced oxygen permeability, which is crucial for extending the shelf life of packaged foods.[27] Researchers are

increasingly focusing on the biodegradability of n-HAP-based packaging. A study by Hadi *et al.* emphasized that n-HAP can be incorporated into biodegradable polymers, promoting a sustainable approach to food packaging while maintaining functionality.[28] Studies have shown that incorporating n-HAP into polymers like polyethylene (PE) and polylactic acid (PLA) improves tensile strength and flexibility. For instance, Zhang *et al.* demonstrated that n-HAP-filled PLA films exhibited a 30% increase in tensile strength compared to pure PLA.[27] Hydroxyapatite presents a promising alternative to other nanomaterials in food packaging due to its unique combination of mechanical reinforcement, barrier properties, biodegradability, and antimicrobial activity. Other nano-materials used for reinforcing packaging are silver nanoparticles (AgNPs),[29] zinc oxide nanoparticles (ZnO),[30] clay nanocomposites,[31] *etc.* Research by Guido *et al.* indicated that AgNPs have superior antimicrobial properties.[32] Similarly, a study by Akram *et al.* demonstrated that ZnO nanocomposites effectively reduce the microbial load on food surfaces, while n-HAP provides better mechanical reinforcement without compromising on flexibility.[33] Clay-infused packaging films reduced gas permeability significantly, while n-HAP combined improved mechanical strength with antimicrobial functionality, making it a more versatile option.[34] These kinds of materials like AgNPs and ZnO offer strong antimicrobial effects, which may raise safety and environmental concerns.[35] In contrast, n-HAP's biocompatibility and effectiveness in enhancing both the structural and functional attributes of food packaging make it a valuable addition to the field.[36]

Starch-based materials have gained attention as potential choices for packaging film due to their abundance, renewability, biodegradability, compatibility with additives, and film-forming ability; however, native starch film has certain drawbacks like poor barrier and mechanical properties. There has been a recent surge in interest in exploiting cassava starch's economic potential for a variety of uses as it is non-toxic, stable, biocompatible, and biodegradable.[37] It has been demonstrated that adding nanosized fillers to the polymer matrix will improve the physical and barrier properties of starch-based and other polymer-based biodegradable packaging.[38] Even though n-HAP studies are mostly concentrated on bone tissue engineering,[39] many researchers[17] have also attempted its application as a reinforcing agent in biodegradable food packaging. n-HAP is found to be biocompatible with enhanced surface area resembling natural apatite.[40] Yao *et al.* used n-HAP and poly(butylene adipate-*co*-butylene terephthalate) (PBAT) as fillers in hydroxyapatite, PBAT, and polylactide (PLA) based composite films.[41] The study demonstrated the capacity of n-HAP to increase the crystallinity of the composite films and regulate the barrier properties.

This present study aims to optimize the preparation of n-HAP from the bone side stream from one of the most common aquaculture species, the *Pangasius* catfish (*Pangasius hypophthalmus*) using the thermal calcination method and characterize its properties such as purity, crystallinity, and particle size. This study further investigates a novel application of n-HAP (as a reinforcing agent in cassava starch-based edible

heat-sealable film) including its mechanical and barrier properties for its suitability as a biodegradable environmentally friendly food packaging material.

2 Materials and methods

2.1 Raw materials

Pangasius catfish frames were collected from the Thoppumpady Fish Harbor, Cochin, India, and transported to the laboratory under chilled conditions (4 ± 2 °C) in an insulated container with ice. The frames were washed thoroughly in potable water at room temperature to remove the adhering tissue, blood, and mucus. The washed bones were dried and packed in polyethylene pouches and stored in a freezer (−18 °C) until further processing. For preparing the edible film, cassava starch (Urban Platter, India), glycerol (Food Grade, Viveka Essence Mart, India), and 5% acetic acid (Food Grade, UMS Food Products, India) were used. Analytical grade acetone and sodium hydroxide (NaOH) were purchased from Merck Ltd. (Mumbai, India).

2.2 Preparation of nano-hydroxyapatite (n-HAP) from *Pangasius* bone side streams

2.2.1 Pre-treatment. The chemical composition of the fishbone was determined by using the association of official analytical chemists AOAC 18th edition (2005).[42] The pre-treatment was performed as per the method suggested by Venkatesan *et al.*[17] The cleaned and stored fish bones were initially boiled in distilled water for 3 h and later drained and again boiled in distilled water (2 g/100 ml H_2O) with 10 ml acetone and 2% NaOH for 1 h. The bones were then washed free of chemicals and dried in a laboratory oven (Kemi, India) at 60 °C for 24 h and stored under dry conditions for further treatment.

2.2.2 Thermal calcination process. The pre-treated fish bone samples were subjected to thermal calcination at three different temperatures of 500, 700, and 900 °C with time combinations of 2, 4, and 9 h for each temperature with a heating rate of 5 °C min^{-1} under ambient conditions in an electric muffle furnace (Nabertherm, Germany). The temperature and time combination for producing n-HAP in this study were selected based on the previous observations made on different fishes. The hydroxyapatite with a Ca/P ratio of about 1.69–1.72 was successfully extracted from snakehead fish (*Channa striata*) bone with a calcination temperature of 600 °C for 5 hours.[43] Higher temperatures produce hydroxyapatite that is more pure and has a higher degree of crystallinity. According to the findings, a sample of black tilapia fish bones that had been calcined at 900 °C had greater intensity than that calcined at 700 °C, with a Ca/P ratio of 1.56.[44] The samples were cooled to room temperature and then pulverized into a fine powder using a lab pulverizer (RETSCH-GmbH-Germany). The obtained product size and microstructure were confirmed by transmission electron microscopy (TEM) (JEOL-JEM210FEG Germany) analysis. Fig. 1 systematically demonstrates the preparation of nano-hydroxyapatite from *Pangasius* catfish bones.

2.3 Characterization of n-HAP

2.3.1 Mineral composition analysis. The mineral composition of the n-HAP produced by thermal calcination at three different temperatures of 500, 700, and 900 °C with time combinations of 2, 4, and 9 h was analyzed using inductively coupled plasma optical emission spectroscopy (ICP-OES) (ICP-OES 7000 series, Thermo Scientific, USA). To 1 g of sample, 10 ml of concentrated nitric acid (HNO_3) and 5 ml of concentrated perchloric acid ($HCLO_4$) (2 : 1) were added and digested at 70 °C. The digested sample was filtered and transferred to a 25 ml standard flask and made up using Milli-Q water. The samples were then analyzed simultaneously with a blank. The results were further utilized to calculate the stoichiometric ratio (Ca/P) of the developed n-HAP.[45]
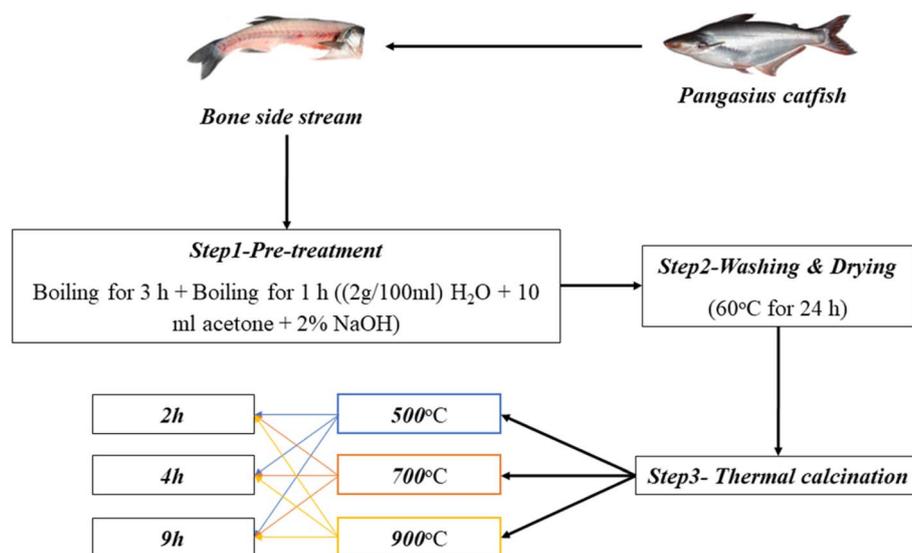

Fig. 1 Process of preparation of nano-hydroxyapatite from *Pangasius* catfish bones.

2.3.2 Fourier-transform infrared spectroscopic (FT-IR) analysis. A Fourier transform infrared spectroscopy system (Shimadzu IR Prestige-21, Japan) equipped with a universal attenuated total reflectance (UATR) accessory was used to study the various functional groups present in n-HAP. The spectra were recorded in the frequency range between 4000 cm^{-1} and 600 cm^{-1} at a resolution of 4 cm^{-1}. The internal reflection crystal made of zinc selenide had a 45° angle of incidence to the IR beam and collected the signals in 32 scans at a resolution of 4 cm^{-1} against a background spectrum recorded from the clean, empty cell at 25 °C. The data is analyzed using the program FT-IR spectrum software. The functional group distributions of n-HAP samples were identified based on the peak values in the region of IR radiation.

2.3.3 X-ray diffraction (XRD) analysis. X-ray powder diffraction (XRD) was used to investigate the crystalline characteristics of the synthesized n-HAP powders. The XRD pattern of the final n-HAP particles was obtained with Cu-Kα radiation ($\lambda = 0.15406$ nm) using a diffractometer (Bruker Avance 370). The XRD patterns were recorded in a 2θ range of 20° to 60°. The current and voltage were set to 40 mV and 40 mA and the data were collected. Hydroxyapatite typically exhibits characteristic diffraction peaks that correspond to its crystalline lattice.

2.3.4 Transmission electron microscopy (TEM) analysis. The morphology and microstructure of n-HAP were examined by using a transmission electron microscope (JEOL-JEM210FEG Germany) equipped with a slow digital scan camera, with a point resolution of 0.23 nm and lattice resolution of 0.14 nm, using an accelerating voltage of 200 kV.

2.4 Preparation of biodegradable film

Edible films were prepared using cassava starch and n-HAP by the solvent casting method with slight modifications.[46] As an inexpensive raw material, starch is a biodegradable natural polymer for creating new advancements for the packaging sector because of its great ability to create inexpensive, gluten-free biodegradable film.[47] The control film was prepared with about 12 g of cassava starch powder (PMW, India) mixed with 100 ml distilled water and gelatinized at 90 °C for 30 minutes with continuous mechanical stirring. Following that, 1.5 ml glycerol and 1 ml of 5% acetic acid were added, and the mixture was stirred at 700 rpm at 70 °C for 15 minutes using a magnetic stirrer (AN-MSH-680, India). 50 ml of this gelatinized mixture was poured and spread using a glass rod onto an area of 17 cm^2 marked on an acrylic sheet and was allowed to dry at 45 °C for 48 hours. For the experimental films, n-HAP powder with the stoichiometric ratio (Ca/P) closest to the standard ratio (1.67) was selected and incorporated into the starch matrix at 4 different concentrations of 0.2%, 0.4%, 0.6% and 0.8%.

2.5 Determination of thickness and mechanical properties of the films

The thickness of the films was determined using a digital micrometer (Model, DC 516, Reed Instruments Ltd., USA). The average of 5 measurements was reported as the mean value. The mechanical properties of the films were measured with a Universal Testing Machine (EZLX Shimadzu, Japan). The films were cut into strips of dimensions 150 mm × 25 mm and were kept for 48 h at 23 °C with 53% relative humidity for conditioning before analysis in accordance with ASTM D882.[48]

2.5.1 Tensile strength and elongation at break. The tensile strength of the films was determined according to ASTM D882.[48] A 1 kN load cell was used with initial grip separation with crosshead speeds of 50 mm s^{-1} and 1 mm s^{-1}. Elongation at break (EB) is a mechanical attribute that indicates the flexibility and elongation potential before the film starts to break. Elongation at break of the films was determined according to ASTM D882.[48] The following equation is used for calculating the value of elongation at break.

$$\% \text{ elongation} = \frac{(L_2 - L_1)}{L_1} \times 100$$

L_1 – original length, L_2 – length at the time of the break.

2.5.2 Young's modulus. Young's modulus (YM) is a dimension of stiffness of the film when attempted to stretch vertically by a tensile force. A low YM value demonstrates that a film has a high elasticity or low stiffness value.[49] It is determined by the elastic slope of the stress–strain graph, which

Table 1 The proximate composition of *Pangasius* fish bone[a]

Parameter (%)	Raw bone	Boiled and cleaned bone
Moisture	51.2 ± 0.56	35.78 ± 0.13
Protein	30.3 ± 1.32	4.2 ± 0.41
Lipid	13 ± 0.34	3.8 ± 0.82
Ash	4.1 ± 0.52	55.1 ± 0.02

[a] Values are indicated as mean ± standard deviation ($n = 3$).

Table 2 Yield and CA/P ratio of n-HAP powder obtained after calcination[a]

Calcination temperature °C	n-HAP yield (%)			CA/P ratio		
	2 h	4 h	9 h	2 h	4 h	9 h
500	66.58 ± 0.12	64.30 ± 0.23	74.5 ± 0.31	1.3 ± 0.27	1.4 ± 0.39	1.40 ± 0.34
700	73.90 ± 0.42	60.32 ± 0.26	68.62 ± 0.43	1.34 ± 0.51	1.4 ± 0.29	1.31 ± 0.33
900	56.68 ± 0.29	52.00 ± 0.51	67.22 ± 0.34	1.33 ± 0.2	1.3 ± 0.22	1.56 ± 0.15

[a] Values are presented as the mean ± standard deviations ($n = 3$).

indicates a material's relative stiffness. The ratio of the stress value to the matching strain value is used for the calculation. This will lead to a proportionality constant called Young's modulus (E), or the modulus of elasticity.[50]

$$E = \frac{\sigma}{\varepsilon}$$

where E is the Young's modulus of the material, σ is the stress applied to the material, and ε is the strain corresponding to applied stress in the material.

2.5.3   Seal strength. Seal strength (SS) could be portrayed as the force required for peeling off two thermally fused layers of polymers. In the food packaging industry, heat sealing is widely used to combine polymer films. The procedure of heat sealing is one where the polymer films are melted at high temperatures and then subjected to pressure thus increasing the interface between hydrogen bonds at the bonding surface accordingly combining two films into one.[22,51,52] The seal strength of the film was determined using a universal testing machine (EZLX Shimadzu, Japan) and trapezium software according to ASTM F88 standards. The individual films were heat sealed using a heat sealing machine (Sevana, India) with a 2 mm seal thickness and impulse heating time of 2 seconds. Each leg of the sealed film sample was clamped to the instrument and vertically fixed in the pulling direction. The distance between the clamps was 50 mm. The seal strength was calculated as follows:

$$\text{Seal strength} = \text{peak force/film width}$$

2.5.4   Water vapor transmission rate (WVTR). The water vapor transmission rate (WVTR) of the films was determined gravimetrically at 25 ± 1 °C using the ASTM E96 method.[53] A container with silica gel was closed with a sample of the experimental film firmly fixed on top. Then the container was placed in a desiccator over a saturated salt solution of potassium iodide (KI) having a known relative humidity of 63.2% RH. The films were weighed daily for 5 days in an analytical balance. The WVTR of the film was determined as follows:

$$\text{WVTR} = G/[t \times A]$$

where WVTR has units of g Pa^{-1} m^{-1} s^{-1}.

The term G/t was calculated by linear regression from the points of weight gain and time, over a constant rate period. A is the area of the exposed films. All the tests were conducted in triplicate.

3   Results and discussion

3.1   Proximate composition

The chemical composition of the fishbone is presented in Table 1. The raw bone has a moisture content, protein, lipid, and ash content of $57.2 \pm 0.56\%$, $30.3 \pm 1.32\%$, $13 \pm 0.34\%$, and $4.1 \pm 0.52\%$, respectively, while that of boiled and cleaned bones was $35.78 \pm 0.13\%$, $4.2 \pm 0.41\%$, $3.8 \pm 0.82\%$, and $55.01 \pm 0.02\%$, respectively. Similar observations were reported in catfish frames where washing, cleaning, and further processing

Table 3 Mineral composition (mg kg^{-1}) of thermally calcined n-HAP powder[a]

	Zn	Pb	Cu	Fe	Ni	Mn	Cr	K	Ba	Na	Ca	P
HAP 500 (2 h)	2.25 ± 0.03^c	0.06 ± 0.03^{abc}	0.04 ± 0.03^{ab}	5.25 ± 0.05^g	0.01 ± 0.01^a	1.73 ± 0.02^c	0.75 ± 0.07^e	11.57 ± 0.08^h	0.75 ± 0.05^c	1.20 ± 0.04^{ab}	1.44 ± 0.03^a	1.04 ± 0.03^d
HAP 700 (2 h)	2.67 ± 0.02^e	0.04 ± 0.02^{ab}	0.03 ± 0.04^a	2.88 ± 0.04^d	0.07 ± 0.04^d	1.81 ± 0.03^{cd}	0.14 ± 0.03^a	6.69 ± 0.04^d	0.96 ± 0.05^e	0.02 ± 0.01^a	1.53 ± 0.02^{bc}	1.19 ± 0.02^a
HAP 900 (2 h)	1.87 ± 0.03^b	0.13 ± 0.05^d	0.09 ± 0.06^{abc}	3.93 ± 0.03^f	0.15 ± 0.04^b	1.46 ± 0.03^b	0.53 ± 0.01^d	8.45 ± 0.07^f	0.65 ± 0.01^b	0.13 ± 0.02^c	$1.65 \pm 0.06^{b-e}$	1.17 ± 0.04^b
HAP 500 (4 h)	1.26 ± 0.05^a	0.10 ± 0.03^{bcd}	0.06 ± 0.06^{abc}	2.69 ± 0.05^c	0.05 ± 0.03^a	1.01 ± 0.08^a	0.31 ± 0.05^b	8.93 ± 0.04^g	0.41 ± 0.01^a	0.13 ± 0.06^b	1.53 ± 0.08^{de}	1.21 ± 0.02^b
HAP 700 (4 h)	1.93 ± 0.05^b	0.08 ± 0.04^{bcd}	0.20 ± 0.01^d	5.20 ± 0.07^g	0.05 ± 0.03^a	1.47 ± 0.01^b	0.73 ± 0.03^e	12.15 ± 0.04^i	0.65 ± 0.01^b	0.17 ± 0.03^{cd}	$1.57 \pm 0.03^{b-e}$	1.17 ± 0.09^{bc}
HAP 900 (4 h)	1.89 ± 0.05^b	0.01 ± 0.00^a	0.04 ± 0.03^{ab}	3.21 ± 0.00^e	0.07 ± 0.04^a	1.82 ± 0.10^d	0.37 ± 0.01^c	2.94 ± 0.06^a	0.82 ± 0.05^d	0.17 ± 0.06^{cd}	1.56 ± 0.04^{bcd}	1.14 ± 0.01^{bc}
HAP 500 (9 h)	2.42 ± 0.00^d	0.07 ± 0.03^{abcd}	0.13 ± 0.03^c	2.27 ± 0.02^b	0.07 ± 0.02^b	1.81 ± 0.04^{cd}	0.24 ± 0.07^b	6.92 ± 0.06^e	0.86 ± 0.10^d	0.21 ± 0.02^a	1.41 ± 0.03^{ab}	1.11 ± 0.06^c
HAP 700 (9 h)	2.87 ± 0.06^f	0.11 ± 0.06^{cd}	0.07 ± 0.05^{abc}	2.15 ± 0.03^a	0.07 ± 0.07^a	1.96 ± 0.03^e	0.31 ± 0.03^{bc}	6.45 ± 0.06^c	0.98 ± 0.08^e	0.22 ± 0.06^{bc}	1.51 ± 0.08^{bc}	1.13 ± 0.04^c
HAP 900 (9 h)	3.78 ± 0.04^g	0.13 ± 0.04^d	0.12 ± 0.04^{bc}	2.83 ± 0.03^d	0.06 ± 0.04^a	2.62 ± 0.03^f	0.36 ± 0.03^c	5.64 ± 0.01^b	1.45 ± 0.02^f	0.21 ± 0.02^e	1.82 ± 0.04^e	1.23 ± 0.04^c

[a] Values are expressed as the mean $\pm$ standard deviation ($n = 3$). Different letters as superscripts in the same column indicate significant differences ($p \leq 0.01$).

significantly reduced moisture and lipid contents and increased ash percentage.[54,55] The considerable reduction in protein is due to the deproteinization steps of boiling and treatment with alkali.[55]

3.2 Yield and mineral composition of n-HAP

The yield of n-HAP powder obtained after calcination is depicted in Table 2. An average n-HAP yield of 52 to 74.5% was reported after calcination. Many studies have reported a similar observation of a reduction in weight with an increase in calcination temperature of around 30 to 40% for sintered fish bone and are described as a result of the decomposition of organic bone components such as fat, collagen, and protein until the major portion remaining is the mineral constituents.[56,57]

The mineral profile analysis is depicted in Table 3. As observed by many researchers in fish bone-derived hydroxyapatite,[58,59] Ca and P were found in higher amounts followed by Fe, Zn, K, and Mn. The stoichiometric ratio (Ca/P) of the extracted n-HAP samples was found to be 1.3 at a calcination temperature of 500 °C for 2 h while it was 1.56 at 900 °C for 9 h, indicating that the n-HAP extracted was non-stoichiometric, which is attributed to the presence of trace amounts of anions and cations integrated into its atomic structure.[60,61]. The Ca/P molar ratio of stoichiometric hydroxyapatite is reported to be 1.67.[62] In this study, a Ca/P ratio close to that of standard hydroxyapatite (1.56) was reported for the sample calcined at a time–temperature combination of 900 °C for 9 h. A similar Ca/P ratio of 1.58 was reported by Akpan *et al.*, with *Pangasius* catfish bones which were calcined at a temperature of 900 °C for 2 h.[22]

3.3 FTIR analysis of n-HAP

The FTIR spectra of n-HAP (Fig. 2) showed absorption peaks at 565.6 cm^{-1}, 599.38 cm^{-1}, and 961.4–1025.3 cm^{-1}, indicating the bending and stretching vibrations of PO_4^{3-}, respectively. The peaks at 873 cm^{-1} and 1410 cm^{-1} indicate the bending mode and stretching vibrations of CO_3^{2-} respectively. This indicates the purity of n-HAP, and it means the collagen and other organic compounds present in the fish bones have been removed by the treatment. Similar absorption peaks were also observed in the FTIR spectra of hydroxyapatite obtained from white-mouth croaker fish.[63]. The bone powder of *Pangasius* sp. was found to contain carbonate and phosphate based on the FT-IR analysis. The carbonate ion presence was indicated by the peaks at 1411.74 as well as the phosphate ion by the strong peaks at 1014.98.[19]

3.4 X-ray diffraction (XRD) analysis of n-HAP

Fig. 3 shows the XRD spectra of n-HAP obtained from catfish bones. The n-HAP exhibits an extremely narrow diffractogram upon calcination, indicating high crystallinity. The XRD results showed the highest intensity peak of the (300) plane, which corresponds to the peak at 32.5°. The positions and intensities of these peaks can vary depending on factors such as crystallinity, purity, and any structural substituents within the hydroxyapatite lattice. The catfish bones calcined at 900 °C exhibit the presence of a main phase of hydroxyapatite together with other minerals that include calcium phosphate, tetracalcium phosphate, tricalcium phosphate, and α-phase calcium phosphate.[22] Sunil *et al.* reported that if the calcium phosphate is lacking in calcium, it is usually converted to tricalcium phosphate at high temperatures (above 650 °C).[64] The crystallinity of the n-HAP obtained from catfish bone powder is 95.5%, indicating the structural properties of hydroxyapatite. This result is in agreement with Akpan *et al.*, who observed that higher crystallinity of 99.9% was found at 900 °C from the same species.[22]
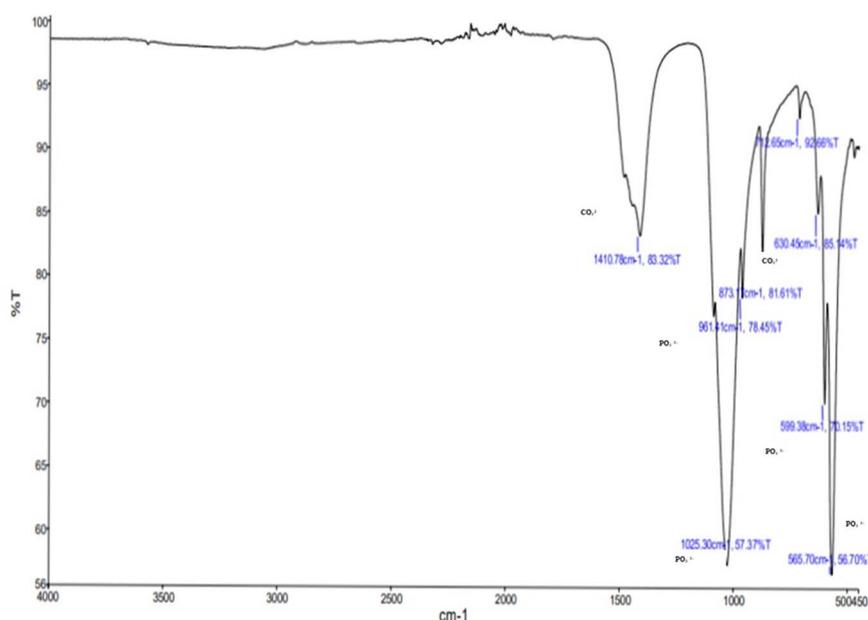

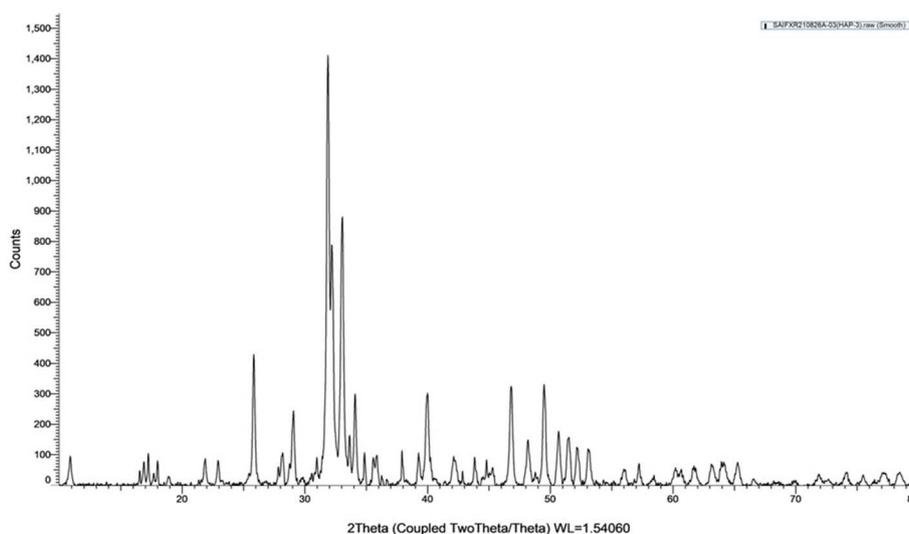Fig. 2 FT-IR vibrational bands of extracted N-HAp (900 °C–9 h).

Fig. 3 X-ray diffraction pattern (XRD) image of n-HAP (900 °C-9 h).

3.5 Transmission electron microscopy (TEM) analysis of n-HAP

The average size of the n-HAP crystals heated at 900 °C was measured to be 71.38 nm. Fig. 4 depicts the transmission electron microscopy image of n-HAP at different scale bars of (a) 100 nm, (b) 50 nm, and (c) 2 nm, and (d) selected area electron diffraction, indicating the crystalline characteristics of n-HAP with a regular spacing and looks like sharp polycrystalline. The nanostructure of n-HAP determined from TEM agrees with Pon-On et al., proving the nanostructure of n-HAP with a latex fringe range of 0.27 nm.[65] Similarly, HAP particles from catfish have a size of 50–70 nm with high porosity and quite good uniformity was observed.[66]

3.6 Film thickness and mechanical properties of the n-HAP incorporating cassava starch biodegradable film

Results of the evaluation of film thickness and mechanical properties of the cassava starch biodegradable film prepared with various concentrations of the n-HAP sample calcined at 900 °C for 9 h with the closest Ca/P ratio (1.57) to the standard ratio are depicted in Table 4.

3.6.1 Film thickness. It was observed that the addition of n-HAP caused slight variations in the film thickness which ranged from 0.05 to 0.16 mm, when compared to the control. Such alterations in thickness are credited to the interface between the polymeric components within the film matrix. After the film formation, these components generate conversion in the segment–segment and segment–chain interactions, particularly between the hydrophilic groups of the polymeric components, decreasing the segment–chain interaction.[67,68] Similarly, Hadi et al. observed that a slight variation in thickness is seen, which may improve the free volume between the starch chains and thicken the film by raising the concentration of hydroxyapatite.[69] Besides, augmented emulsion viscosity and non-homogeneous allotment of the solids per cm² of drying

surface are also indicated as the reason behind this change in final thickness.[70]

3.6.2 Tensile strength. The control film exhibited a TS value of 12.5 MPa while the maximum TS value of 16.10 MPa was exhibited by the sample with 0.8% n-HAP. It was observed that the addition of n-HAP caused a considerable increase in the film's tensile strength. Miculescu et al. reported that for gelatinized starch, a very low amount of hydroxyapatite particles (0.05%) could increase the strength and bioactivity.[71] The results are in accordance with Upadhyay et al.,[72] who reported that increasing the content of hydroxyapatite improves tensile strength.[67]

3.6.3 Elongation at break. The lowest EB values were reported for the control film (CNT) (1.55%) and the maximum (6.87%) was reported for the sample with 0.4% n-HAP (B) followed by the sample with 0.2% n-HAP (6.8%) (A). The results are comparable with those of Okuda et al., who reported that the percentage of elongation at break of hydroxyapatite-incorporated cassava starch films was in the range of 1.7–4.3%, which indicated that the phosphate groups from hydroxyapatite and starch made the composite less fragile.[46] Yu et al. also reported that the elongation at break decreased gradually with the increasing amount of hydroxyapatite.[73] The EB values gradually decreased when the concentration of n-HAP was increased from 0.4% to 0.8% which could be attributed to the brittleness and stiffness of n-HAP. The statistical evaluation showed that all the values were significantly different ($p \leq 0.05$.)

3.6.4 Young's modulus. The study showed that the value of the YM increased from 6.30 to 11.34 MPa as the percentages of n-HAP increased. A film with 0.8% n-HAP has the highest YM (11.34 MPa). Similar results were reported by Okuda et al. that the YM values of the cassava starch-hydroxyapatite composites increased with an increase in n-HAP.[44] Miculescu etal.[71] also made similar observations in this regard stating that when a ceramic phase is added to a composite, the YM increases while
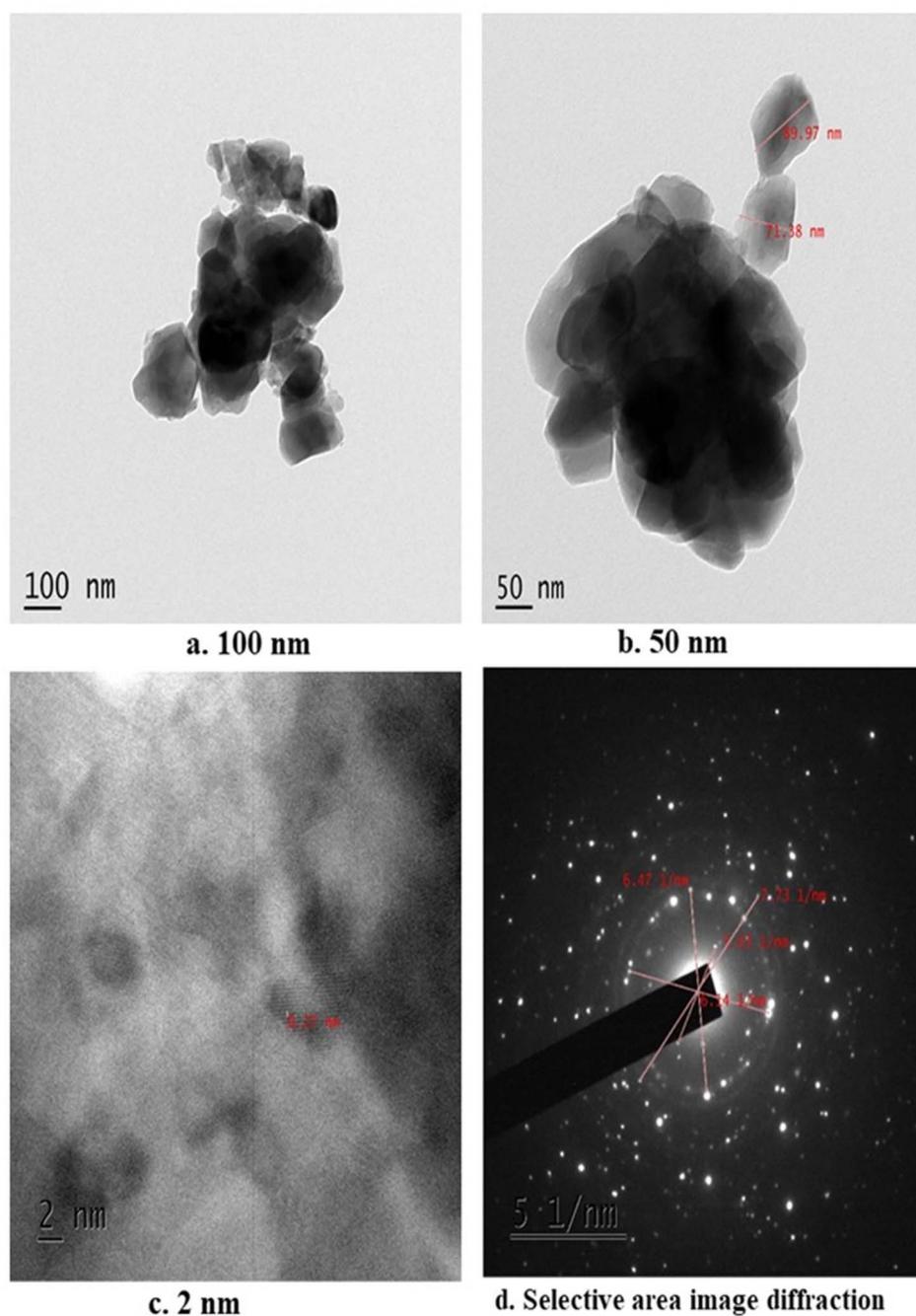
Fig. 4   Transmission electron microscopy (TEM) image of n-HAP (900 °C-9 h) at different scale bars.

Table 4   Mechanical properties and WVTR of the n-HAP incorporating cassava starch biodegradable film[a]

	Thickness (mm)	Tensile strength (MPa)	Elongation at break (%)	Young's modulus (MPa)	Seal strength (N mm^{-1})	WVTR (g Pa^{-1} m^{-1} s^{-1})
Control	0.05 ± 0.001^a	12.50 ± 0.74^a	1.55 ± 0.10^a	6.30 ± 0.93^a	0.67 ± 0.20^a	3.84 ± 0.65^c
A 0.2%	0.05 ± 0.01^a	12.99 ± 0.87^a	6.80 ± 0.60^a	6.41 ± 1.01^a	2.36 ± 0.72^b	3.77 ± 0.22^c
B 0.4%	0.06 ± 0.01^a	13.69 ± 1.22^{ab}	6.87 ± 0.42^a	8.30 ± 1.45^{ab}	2.00 ± 0.22^b	2.40 ± 0.10^b
C 0.6%	0.15 ± 0.03^b	13.69 ± 2.36^{ab}	2.54 ± 1.63^b	8.63 ± 3.37^{ab}	1.31 ± 0.13^a	1.62 ± 0.05^a
D 0.8%	0.16 ± 0.02^b	16.10 ± 1.86^b	2.10 ± 1.22^b	11.34 ± 1.88^b	2.65 ± 0.12^b	2.08 ± 0.18^{ab}

[a] Values are expressed as the mean $\pm$ standard deviation ($n = 3$). Different letters in the same column indicate significant differences ($p \leq 0.05$).

the ductility of the material decreases, as observed in composites made of hydroxyapatite and starch.[66]

3.6.5   Seal strength. It was observed that the seal strength of the starch–n-HAP composite increased significantly compared to that of the control. This could be due to the intermolecular bond between starch and n-HAP particles, which can reduce the moisture content. The film incorporating 0.8% n-HAP showed the highest seal strength. The increase in seal strength at lower concentrations of n-HAP (0.2% and 0.4%) could be due to the reinforcement effect provided by the nano-hydroxyapatite particles, which might enhance the film's mechanical properties by providing better cross-linking or filler effects.[74] The drop at 0.6% may indicate agglomeration of n-HAP particles, which could cause structural imperfections or weak points in the film, leading to reduced seal strength.[75] The recovery of seal strength at 0.8% might be attributed to a better distribution of n-HAP at higher concentrations or a critical concentration where the particles are sufficiently dispersed to again reinforce the film structure.[76]

3.6.6   Water vapor transmission rate (WVTR). In the study (Table 4) it was observed that the WVTR of composite films reduced as n-HAP concentration increased. The control film showed the highest value (3.84 ± 0.65) and was significantly different from n-HAP incorporating films ($p < 0.05$). The film incorporating 0.2% n-HAP was not significantly different from the control film (3.77 ± 0.22) as the film had low n-HAP concentration. The film incorporating 0.4% n-HAP showed identical values to that of the film incorporating 0.8% n-HAP. A percentage reduction of 42% in WVTR was observed between the control and the film sample with 0.6% n-HAP. A similar percentage (34%) reduction was observed by Gupta *et al.*, with 2.5% n-HAP incorporated in the polylactic acid film.[77] Notably, the water vapour barrier was greatly enhanced when n-HAP was added to the edible bio-film. It is believed that the presence of n-HAP contributed to the tightening of the network structure and the decrease of porosity and space in the film matrix, which limited the transport of water vapor.[78]

4   Conclusion

The study successfully demonstrated that the thermal calcination method could be utilized for the conversion of the *Pangasius* catfish bone side stream into nano-sized hydroxyapatite (n-HAP) with a moderately lower stoichiometric ratio with standard hydroxyapatite. The calcination of fish bone resulted in the formation of n-HAP with a Ca/P ratio of 1.56 at 900 °C for 9 h with a crystallinity of 95.5%. In addition to this, the derived n-HAP showed a nanostructure of 71.38 nm crystals at 900 °C. The study also demonstrated a novel application of n-HAP as a structural component of cassava starch-based biodegradable film. It was observed that the addition of n-HAP caused a slight increase in the film thickness when compared to the control. The physical properties such as tensile strength (TS), elongation at break, and seal strength significantly increased with the incorporation of n-HAP. Water vapour transmission rate (WVTR), which is one of the crucial barrier properties considered for evaluating films for food packaging applications also

significantly reduced by n-HAP addition making the film more impermeable to moisture. Considering the physical and barrier properties of the n-HAP incorporating cassava starch film, an n-HAP concentration of 0.8% was observed to be ideal for the film application. The study demonstrates that addition of n-HAP could significantly improve the value of casava starch as a suitable material for the development of efficient biodegradable packaging solutions for the food industry against the plastic counterparts.

Data availability

The authors confirm that the data supporting the findings of this study are available within the article.

Author contributions

Thool Oshin Kawduji – writing – original draft, Abhilash Sasidharan – review and editing, visualization, data curation, project administration, investigation, supervision, Sarasan Sabu – formal analysis, Muhammed Navaf – visualisation, analysis, Kappat Valiyapeediyekkal Sunooj – review and editing.

Conflicts of interest

The authors declare no conflict of interest.

References

1 F. Ozogul, M. Cagalj, V. Šimat, Y. Ozogul, J. Tkaczewska, A. Hassoun, A. A. Kaddour, E. Kuley, N. B. Rathod and G. G. Phadke, Recent developments in valorisation of bioactive ingredients in discard/seafood processing by-products, *Trends Food Sci. Technol.*, 2021, **116**, 559–582.

2 A. E. Ghaly, V. V. Ramakrishnan, M. S. Brooks, S. M. Budge and D. Dave, Fish processing wastes as a potential source of proteins. Amino acids and oils: a critical review, *J. Microb. Biochem. Technol.*, 2013, **5**(4), 107–129.

3 T. Maschmeyer, R. Luque and M. Selva, Upgrading of marine (fish and crustaceans) biowaste for high added-value molecules and bio (nano)-materials, *Chem. Soc. Rev.*, 2020, **49**(13), 4527–4563.

4 A. L. Välimaa, S. Mäkinen, P. Mattila, P. Marnila, A. Pihlanto, M. Mäki and J. Hiidenhovi, Fish and fish side streams are valuable sources of high-value components, *Food Qual. Saf.*, 2019, **3**(4), 209–226.

5 Action S. I., *World Fisheries and Aquaculture*, Food and Agriculture Organization, 2020, **2020**, pp. 1–244.

6 V. Wankhade, Animal-derived biopolymers in food and biomedical technology, in *Biopolymer-based Formulations*, Elsevier, 2020, pp. 139–152.

7 S. M. Chisenga, G. N. Tolesa and T. S. Workneh, Biodegradable food packaging materials and prospects of the fourth industrial revolution for tomato fruit and product handling, *Int. J. Food Sci.*, 2020, **2020**(1), 8879101.

8 M. U. Munir, S. Salman, I. Javed, S. N. Bukhari, N. Ahmad, N. A. Shad and F. Aziz, Nano-hydroxyapatite as a delivery

system: overview and advancements, *Artif. Cells, Nanomed., Biotechnol.*, 2021, **49**(1), 717–727.

9 T. P. Wendari, S. Ramadani, Y. Stiadi and N. Sofyan, CuFe2O4/hydroxyapatite magnetic nanocomposite synthesized using pensi clam shells as a source of calcium for degradation of dye and anti-bacterial applications, *Case Stud. Chem. Environ. Eng.*, 2023, **8**, 100482.

10 S. Balhuc, R. Campian, A. Labunet, M. Negucioiu, S. Buduru and A. Kui, Dental applications of systems based on hydroxyapatite nanoparticles—an evidence-based update, *Crystals*, 2021, **11**(6), 674.

11 N. Kumar, S. Ali, B. Kumar, M. S. Zafar and Z. Khurshid, Hydroxyapatite and nanocomposite implant coatings, in *Dental Implants*, Woodhead Publishing, 2020, pp. 69–92.

12 M. R. M. Roslan, N. L. M. Kamal, M. F. A. Khalid, N. F. M. Nasir, E. M. Cheng, C. Y. Beh, J. S. Tan and M. S. Mohamed, The state of starch/hydroxyapatite composite scaffold in bone tissue engineering with consideration for dielectric measurement as an alternative characterization technique, *Materials*, 2021, **14**(8), 1960.

13 I. N. Amirrah, Y. Lokanathan, I. Zulkiflee, M. M. Wee, A. Motta and M. B. Fauzi, A comprehensive review on collagen type I development of biomaterials for tissue engineering: from biosynthesis to bioscaffold, *Biomedicines*, 2022, **10**(9), 2307.

14 D. Coppola, C. Lauritano, F. P. Esposito, G. Riccio, C. Rizzo and D. de Pascale, Fish waste: from problem to valuable resource, *Mar. Drugs*, 2021, **19**(2), 116.

15 H. Z. Abdullah, M. I. Idris, L. Te Chuan, S. K. Dermawan and M. Z. Jaffri, Natural Hydroxyapatite from Black Tilapia Fish Bones and Scales for Biomedical Applications, in *Sustainable Material for Biomedical Engineering Application*, Springer Nature Singapore, Singapore, 2023, pp. 107–124.

16 D. R. Sahoo and T. Biswal, Synthesis and optimization of properties of poly(AN-co-AA)/fish bone biocomposite by using artificial neural networks, *Polym. Bull.*, 2023, **80**(6), 6545–6565.

17 J. Venkatesan and S. K. Kim, Effect of temperature on isolation and characterization of hydroxyapatite from tuna (Thunnus obesus) bone, *Materials*, 2010, **3**(10), 4761–4772.

18 A. Pamungkas, R. Dhelika and A. S. Saragih, Synthesis of hydroxyapatite from Tenggiri (Scomberomorus commersonii) fish bone: findings on experiment and processes, in *AIP Conference Proceedings*, AIP Publishing, 2019, vol. 2092, no. 1.

19 H. Novianty, A. R. Sefrienda and J. Jasmadi, Analyzing the Characteristics of Fishbone Powder Derived from Pangasius sp., Thunnus tonggol, and Thunnus albacares as Food Fortificant, *agriTECH*, 2024, **44**(1), 90–100.

20 F. S. Kibenge, Introduction to aquaculture and fisheries, in *Aquaculture Virology*, Academic Press, 2016, pp. 3–8.

21 P. L. Hariani and M. Said, Effect of sintering on the mechanical properties of hydroxyapatite from fish bone (Pangasius Hypophthalmus), *IOP Conf. Ser.: Mater. Sci. Eng.*, 2019, **509**(1), 012109.

22 E. S. Akpan, M. Dauda, L. S. Kuburi and D. O. Obada, A facile synthesis method and fracture toughness evaluation of catfish bones-derived hydroxyapatite, *MRS Adv.*, 2020, **5**, 1357–1366.

23 W. R. Wulan and N. A. Fauziyah, Overview of the use of the sol-gel method in the synthesis and analysis of hydroxyapatide from biowaste, *J. Phys.: Conf. Ser.*, 2024, **2780**(1), 012023.

24 H. Yamamura, V. H. da Silva, P. L. Ruiz, V. Ussui, D. R. Lazar, A. C. Renno and D. A. Ribeiro, Physico-chemical characterization and biocompatibility of hydroxyapatite derived from fish waste, *J. Mech. Behav. Biomed. Mater.*, 2018, **80**, 137–142.

25 A. Salian, A. K. Prakash, G. Gulladi, S. Andiappan, V. K. Surasani and R. C. Varadaraju, Valorization of emperor fish (Lethrinus fraenatus) filleting waste in to fishbone hydroxyapatite by thermal calcination method, *Biomass Convers. Biorefin.*, 2024, **24**, 1–8.

26 F. Fendi, B. Abdullah, S. Suryani, I. Raya and D. Tahir, The use of waste bones of rabbitfish (Siganus sp.) for the synthesis of hydroxyapatite, *IOP Conf. Ser. Earth Environ. Sci.*, 2023, **1230**(1), 012042.

27 R. Zhang and H. Xu, Environmental properties and applications of cellulose and chitin-based bionanocomposites, in *Biodegradable and Environmental Applications of Bionanocomposites*, Springer International Publishing, Cham, 2022, pp. 99–140.

28 Z. Hadi, N. Hekmat and F. Soltanolkottabi, Effect of hydroxyapatite on physical, mechanical, and morphological properties of starch-based bio-nanocomposite films, *Compos. Adv. Mater.*, 2022, **31**, DOI: 10.1177/26349833221087755.

29 K. Kraśniewska, S. Galus and M. Gniewosz, Biopolymers-based materials containing silver nanoparticles as active packaging for food applications–a review, *Int. J. Mol. Sci.*, 2020, **21**(3), 698.

30 N. Coneo, Y. Ramos, G. De Ávila, A. Herrera and A. Cremades, Active chitosan-poly (vinyl alcohol) film reinforced with zinc oxide nanoparticles for food packaging applications, *Polym. Renew. Resour.*, 2023, **14**(3), 173–194.

31 R. K. Deshmukh, L. Hakim, K. Akhila, D. Ramakanth and K. K. Gaikwad, Nano clays and its composites for food packaging applications, *Int. Nano Lett.*, 2023, **13**(2), 131–153.

32 Z. N. Guido, M. V. Braum, N. M. Possolli, R. De Bonna, L. V. Ponsoni, M. K. de Almeida, E. Angioletto and M. V. Zimmermann, *Part 2: The Effect of Functionalizing Silica Gel with Ag and ZnO Nanoparticles on Antimicrobial Properties and Their Application in Meat Packaging*, available at SSRN 4956871.

33 W. Akram, R. Zahid, R. M. Usama, S. A. AlQahtani, M. Dahshan, M. A. Basit and M. Yasir, Enhancement of antibacterial properties, surface morphology and in vitro bioactivity of hydroxyapatite-zinc oxide nanocomposite coating by electrophoretic deposition technique, *Bioengineering*, 2023, **10**(6), 693.

34 R. Zhang and H. Xu, Environmental properties and applications of cellulose and chitin-based bionanocomposites, in *Biodegradable and Environmental*

Applications of Bionanocomposites, Springer International Publishing, Cham, 2022, pp. 99–140.

35 M. Khan, M. S. Khan, K. K. Borah, Y. Goswami, K. R. Hakeem and I. Chakrabartty, The potential exposure and hazards of metal-based nanoparticles on plants and environment, with special emphasis on ZnO NPs, TiO2 NPs, and AgNPs: a review, *Environ. Adv.*, 2021, **6**, 100128.

36 N. H. Sari, M. Z. Rivlan, S. Suteja, H. Kadriyan and S. M. Thiagamani, A Review on Silver Nanoparticles Based Biomaterials for Bone Tissue Engineering and Medical Applications, *Indones. J. Chem.*, 2024, **24**(4), DOI: [10.22146/ijc.92830](10.22146/ijc.92830).

37 F. Haq, H. Yu, L. I. Wang, L. Teng, M. Haroon, R. U. Khan, S. Mehmood, R. S. Ullah, A. Khan and A. Nazir, Advances in chemical modifications of starches and their applications, *Carbohydr. Res.*, 2019, **476**, 12–35.

38 K. Y. Perera, M. Hopkins, A. K. Jaiswal and S. Jaiswal, Nanoclays-containing bio-based packaging materials: properties, applications, safety, and regulatory issues, *J. Nanostructure Chem.*, 2024, **14**(1), 71–93.

39 M. R. M. Roslan, N. L. M. Kamal, M. F. A. Khalid, N. F. M. Nasir, E. M. Cheng, C. Y. Beh, J. S. Tan and M. S. Mohamed, The state of starch/hydroxyapatite composite scaffold in bone tissue engineering with consideration for dielectric measurement as an alternative characterization technique, *Materials*, 2021, **14**(8), 1960.

40 F. Damiri, A. Fatimi, A. M. Musuc, A. C. Santos, S. Paszkiewicz, C. I. Idumah, S. Singh, R. S. Varma and M. Berrada, Nano-hydroxyapatite (nHAp) scaffolds for bone regeneration: preparation, characterization and biological applications, *J. Drug Delivery Sci. Technol.*, 2024, 105601.

41 Q. Yao, Z. Song, J. Li and L. Zhang, Micromorphology, mechanical, crystallization and permeability properties analysis of HA/PBAT/PLA (HA, hydroxyapatite; PBAT, poly (butylene adipate-co-butylene terephthalate); PLA, polylactide) degradability packaging films, *Polym. Int.*, 2020, **69**(3), 301–307.

42 AOAC, Association of Official Analytical Chemist, *Official Methods of Analysis*, AOAC International, Suite 500, 481 North Frederick Avenue, Gaithersburg, Maryland 20877-2417, USA, 18th edn, 2005.

43 I. Widiastuti and S. Sudirman, Hydroxyapatite characteristics from snakehead fish (Channa striata) bone via alkali treatment followed by calcination method, *Trop. J. Nat. Prod. Res.*, 2024, **8**(2), 6147–6151.

44 S. K. Dermawan, Z. M. Ismail, M. Z. Jaffri and H. Z. Abdullah, Effect of the calcination temperature on the properties of hydroxyapatite from black tilapia fish bone, *J. Phys.: Conf. Ser.*, 2022, **2169**(1), 012034.

45 P. V. Nam, N. Van Hoa and T. S. Trung, Properties of hydroxyapatites prepared from different fish bones: a comparative study, *Ceram. Int.*, 2019, **45**(16), 20141–20147.

46 Y. Okuda, K. Hirota, T. Mizutani and Y. Aoyama, Co-precipitation of tapioca starch and hydroxyapatite. Effects of phosphorylation of starch on mechanical properties of the composites, *Results Mater.*, 2019, **3**, 100035.

47 H. Onyeaka, K. Obileke, G. Makaka and N. Nwokolo, Current research and applications of starch-based biodegradable films for food packaging, *Polymers*, 2022, **14**(6), 1126; N. Donati, J. C. Spada and I. C. Tessaro, Recycling rice husk ash as a filler on biodegradable cassava starch-based foams, *Polym. Bull.*, 2023, **80**(9), 10231–10248.

48 ASTM D 882-02, *Standard Test Method for Tensile Properties of Thin Plastic Sheeting*.

49 S. H. Othman, N. A. Majid, I. S. Tawakkal, R. K. Basha, N. Nordin and R. A. Shapi'I, Tapioca starch films reinforced with microcrystalline cellulose for potential food packaging application, *Food Sci. Technol.*, 2019, **39**, 605–612.

50 A. Vaidya and K. Pathak, Mechanical stability of dental materials, in *Applications of Nanocomposite Materials in Dentistry*, Woodhead Publishing, 2019, pp. 285–305.

51 W. S. Lim, S. Y. Ock, G. D. Park, I. W. Lee, M. H. Lee and H. J. Park, Heat-sealing property of cassava starch film plasticized with glycerol and sorbitol, *Food Packag. Shelf Life*, 2020, **26**, 100556.

52 P. Tongnuanchan, S. Benjakul, T. Prodpran, S. Pisuchpen and K. Osako, Mechanical, thermal and heat sealing properties of fish skin gelatin film containing palm oil and basil essential oil with different surfactants, *Food Hydrocolloids*, 2016, **56**, 93–107.

53 ASTM E96, *Standard Test Methods for Water Vapor Transmission of Materials*.

54 A. Pérez, M. Ruz, P. García, P. Jiménez, P. Valencia, C. Ramírez, M. Pinto, S. M. Nuñez, J. W. Park and S. Almonacid, Nutritional Properties of Fish Bones: Potential Applications in the Food Industry, *Food Rev. Int.*, 2024, **40**(1), 79–91.

55 A. Cahyanto, E. Kosasih, D. Aripin and Z. Hasratiningsih, Fabrication of hydroxyapatite from fish bones waste using reflux method, *IOP Conf. Ser.: Mater. Sci. Eng.*, 2017, **172**(1), 012006.

56 J. A. Lolo, D. P. Ambali, W. Jefriyanto, D. Handayani, W. Afridah, E. A. Wikurendra, R. Amalia and A. Syafiuddin, Synthesis and characterization of hydroxyapatite derived from milkfish bone by simple heat treatments, *Biointerface Res. Appl. Chem.*, 2022, **12**(2), 2440.

57 M. K. Horta, C. Westin, D. N. Rocha, J. B. Campos, R. F. Souza, M. S. Aguilar and F. J. Moura, Hydroxyapatite from biowaste for biomedical applications: obtainment, characterization and in vitro assays, *Mater. Res.*, 2023, **26**, e20220466.

58 Z. Evis, B. Yilmaz, M. Usta and S. L. Aktug, X-ray investigation of sintered cadmium doped hydroxyapatites, *Ceram. Int.*, 2013, **39**(3), 2359–2363.

59 H. Esfahani, E. Salahi, A. Tayebifard, M. R. Rahimipour and M. Keyanpour-Rad, Structural and morphological analysis of zinc incorporated non-stoichiometric hydroxyapatite nano powders, *Matéria*, 2016, **21**, 569–576.

60 M. Vallet-Regi and D. A. Navarrete, Biological apatites in bone and teeth, *Nanoceramics in Clinical Use: From Materials to Applications*, ed. M. Vallet-Regi and D. Arcos Navarrete, 2nd edn, 2015, pp. 1–29.

61 R. Z. LeGeros, Biological and synthetic apatites, in *Hydroxyapatite and Related Materials*, CRC Press, 2017, pp. 3–28.

62 S. Natasha, A. N. Natasha, C. Y. Tan, L. T. Bang, A. Niakan, J. Purbolaksono, H. Chandran, C. Y. Ching and W. D. Teng, Characteristics and properties of hydoxyapatite derived by sol–gel and wet chemical precipitation methods, *Ceram. Int.*, 2015, **41**(9), 10434–10441.

63 H. Yamamura, V. H. da Silva, P. L. Ruiz, V. Ussui, D. R. Lazar, A. C. Renno and D. A. Ribeiro, Physico-chemical characterization and biocompatibility of hydroxyapatite derived from fish waste, *J. Mech. Behav. Biomed. Mater.*, 2018, **80**, 137–142.

64 B. R. Sunil and M. Jagannatham, Producing hydroxyapatite from fish bones by heat treatment, *Mater. Lett.*, 2016, **185**, 411–414, DOI: 10.1016/j.matlet.2016.09.039.

65 W. Pon-On, P. Suntornsaratoon, N. Charoenphandhu, J. Thongbunchoo, N. Krishnamra and I. M. Tang, Hydroxyapatite from fish scale for potential use as bone scaffold or regenerative material, *Mater. Sci. Eng., C*, 2016, **62**, 183–189.

66 P. V. Nam, N. Van Hoa, T. T. Anh and T. S. Trung, Towards zero-waste recovery of bioactive compounds from catfish (Pangasius hypophthalmus) by-products using an enzymatic method, *Waste Biomass Valorization*, 2020, **11**, 4195–4206.

67 E. Basiak, S. Galus and A. Lenart, Characterisation of composite edible films based on wheat starch and whey-protein isolate, *Int. J. Food Sci. Technol.*, 2015, **50**(2), 372–380.

68 S. H. Othman, Bio-nanocomposite materials for food packaging applications: types of biopolymer and nano-sized filler, *Agriculture and Agricultural Science Procedia*, 2014, **2**, 296–303.

69 Z. Hadi, N. Hekmat and F. Soltanolkottabi, Effect of hydroxyapatite on physical, mechanical, and morphological properties of starch-based bio-nanocomposite films, *Compos. Adv. Mater.*, 2022, **31**, DOI: 10.1177/26349833221087755.

70 D. J. McClements and S. M. Jafari, Improving emulsion formation, stability and performance using mixed emulsifiers: a review, *Adv. Colloid Interface Sci.*, 2018, **251**, 55–79.

71 F. Miculescu, A. C. Mocanu, C. A. Dascălu, A. Maidaniuc, D. Batalu, A. Berbecaru, S. I. Voicu, M. Miculescu, V. K. Thakur and L. T. Ciocan, Facile synthesis and characterization of hydroxyapatite particles for high value nanocomposites and biomaterials, *Vacuum*, 2017, **146**, 614–622.

72 P. Upadhyay and A. Ullah, Enhancement of mechanical and barrier properties of chitosan-based bionanocomposites films reinforced with eggshell-derived hydroxyapatite nanoparticles, *Int. J. Biol. Macromol.*, 2024, **261**, 129764.

73 Z. Yu, F. K. Alsammarraie, F. X. Nayigiziki, W. Wang, B. Vardhanabhuti, A. Mustapha and M. Lin, Effect and mechanism of cellulose nanofibrils on the active functions of biopolymer-based nanocomposite films, *Food Res. Int.*, 2017, **99**, 166–172.

74 M. Subramaniyan, S. Karuppan, S. Helaili and I. Ahmad, Structural, mechanical, and in vitro characterization of hydroxyapatite loaded PLA composites, *J. Mol. Struct.*, 2024, **1306**, 137862.

75 Y. Sun, Y. Wang, C. Ji, J. Ma and B. He, The impact of hydroxyapatite crystal structures and protein interactions on bone's mechanical properties, *Sci. Rep.*, 2024, **14**, 9786.

76 U. Lu, W. Dong, J. Ding, W. Wang and A. Wang, 10 - Hydroxyapatite Nanomaterials: Synthesis, Properties, and Functional Applications, in *Micro and Nano Technologies, Nanomaterials from Clay Minerals*, ed. A. Wang and W. Wang, Elsevier, 2019, pp. 485–536.

77 A. Gupta, A. Prasad, N. Mulchandani, M. Shah, M. R. Sankar, S. Kumar and V. Katiyar, Multifunctional nanohydroxyapatite-promoted toughened high-molecular-weight stereocomplex poly (lactic acid)-based bionanocomposite for both 3D-printed orthopedic implants and high-temperature engineering applications, *ACS Omega*, 2017, **2**(7), 4039–4052.

78 S. Choudhary, K. Sharma, P. K. Mishra, V. Kumar and V. Sharma, Development and characterization of biodegradable agarose/gum neem/nanohydroxyapatite/ polyoxyethylene sorbitan monooleate based edible bio-film for applications towards a circular economy, *Environ. Technol. Innov.*, 2023, **29**, 103023.